Photodissociation dynamics of nitromethane and methyl nitrite by infrared multiphoton dissociation imaging with quasiclassical trajectory calculations: Signatures of the roaming pa…

ARTICLE *in* THE JOURNAL OF CHEMICAL PHYSICS · FEBRUARY 2014

Impact Factor: 2.95 · DOI: 10.1063/1.4862691 · Source: PubMed

6 AUTHORS, INCLUDING:

Arghya Dey
Radboud University Nijmegen
17 PUBLICATIONS **55** CITATIONS
SEE PROFILE

Ravin Fernando
University of Missouri
8 PUBLICATIONS **17** CITATIONS
SEE PROFILE

Zahra Homayoon
Emory University
18 PUBLICATIONS **93** CITATIONS
SEE PROFILE

Joel M Bowman
Emory University
541 PUBLICATIONS **14,741** CITATIONS
SEE PROFILE

Photodissociation dynamics of nitromethane and methyl nitrite by infrared multiphoton dissociation imaging with quasiclassical trajectory calculations: Signatures of the roaming pathway

Arghya Dey, Ravin Fernando, Chamara Abeysekera, Zahra Homayoon, Joel M. Bowman, and Arthur G. Suits

Citation: The Journal of Chemical Physics **140**, 054305 (2014); doi: 10.1063/1.4862691
View online: http://dx.doi.org/10.1063/1.4862691
View Table of Contents: http://scitation.aip.org/content/aip/journal/jcp/140/5?ver=pdfcov
Published by the AIP Publishing

Photodissociation dynamics of nitromethane and methyl nitrite by infrared multiphoton dissociation imaging with quasiclassical trajectory calculations: Signatures of the roaming pathway

Arghya Dey,[1] Ravin Fernando,[1] Chamara Abeysekera,[1] Zahra Homayoon,[2] Joel M. Bowman,[2] and Arthur G. Suits[1,a)]
[1]*Department of Chemistry, Wayne State University, Detroit, Michigan 48202, USA*
[2]*Department of Chemistry and Cherry L. Emerson Center for Scientific Computation, Emory University, Atlanta, Georgia 30322, USA*

(Received 28 October 2013; accepted 7 January 2014; published online 3 February 2014)

We combine the techniques of infrared multiphoton dissociation (IRMPD) with state selective ion imaging to probe roaming dynamics in the unimolecular dissociation of nitromethane and methyl nitrite. Recent theoretical calculations suggest a "roaming-mediated isomerization" pathway of nitromethane to methyl nitrite prior to decomposition. State-resolved imaging of the NO product coupled with infrared multiphoton dissociation was carried out to examine this unimolecular decomposition near threshold. The IRMPD images for the NO product from nitromethane are consistent with the earlier IRMPD studies that first suggested the importance of an isomerization pathway. A significant Λ-doublet propensity is seen in nitromethane IRMPD but not methyl nitrite. The experimental observations are augmented by quasiclassical trajectory calculations for nitromethane and methyl nitrite near threshold for each dissociation pathway. The observation of distinct methoxy vibrational excitation for trajectories from nitromethane and methyl nitrite dissociation at the same total energy show that the nitromethane dissociation bears a nonstatistical signature of the roaming isomerization pathway, and this is possibly responsible for the nitromethane Λ-doublet propensity as well. [http://dx.doi.org/10.1063/1.4862691]

INTRODUCTION

The advent of infrared multiphoton dissociation (IRMPD) in the early 1970s has been important in advancing the study of nascent photofragments originating from dissociation of small molecules on the ground electronic state.[1] Initially, trapped-ion mass spectrometry was coupled with IRMPD to study the properties of charged species.[2,3] It has also been employed more recently in determining the sequence of proteins by mass spectrometry.[4] With the introduction of powerful transversely excited atmospheric-carbon dioxide (TEA-CO_2) lasers, IRMPD became a unique tool for studying unimolecular dissociation. It has been used extensively to study reactions that involve concerted pathways as well as tight transition states and simple bond rupture. Lee and co-workers have combined IRMPD with photofragment translational spectroscopy to study the different reaction pathways originating from the unimolecular decomposition of several small molecules such as acetone,[5] acetic acid,[6] and esters.[7] Study of the products revealed several competing processes, such as radical formation, isomerization, and formation of cyclic transition states. Rapid absorption of many infrared photons leads to dissociation of the molecule near the dissociation threshold. This assists in precise mapping of the multidimensional potential energy surface and aids in interpreting the distribution of final products in case of multiple pathways. Experimental findings show that since IRMPD mainly follows the lowest energy pathway, the products formed often resemble those of thermal decomposition.[8,9] However, the main advantage of IRMPD over thermal decomposition is that IRMPD experiments can be carried out in a collision-free environment, so that the primary reaction products may be detected.

Roaming reactions are a newly reported class of unimolecular reactions that involve near-dissociation to radical products followed by abstraction or isomerization leading to distinct and sometimes unexpected products.[10,11] Roaming was initially reported in formaldehyde photodissociation and has since been seen in many systems.[12] Roaming-mediated isomerization has been invoked in dissociation of nitrobenzene[13] and nitromethane[14–16] to account for the significant yield of the NO loss channel in these systems. To-date, however, in primary photodissociation studies of roaming dynamics, only UV excitation has been used to prepare excited molecules for subsequent investigation. Since reactions involving roaming mechanisms largely arise from the ground electronic state, IRMPD studies can be very helpful in providing unambiguous information about such processes.

Nitromethane (CH_3NO_2) is the simplest homologue in the family of nitroalkanes that have been important as energetic materials in the form of propellants and explosives. The photodissociation dynamics of nitromethane have drawn significant attention and have been studied extensively using ultraviolet excitation from the ground electronic state.[17–19] A key early photofragment translational spectroscopy study by

a)Electronic mail: asuits@wayne.edu

Wodtke, Lee and co-workers using IRMPD[20] reported 40% branching to NO loss. This large percentage implied efficient isomerization to the nitrite prior to dissociation:

$$CH_3NO_2 + nhv \rightarrow CH_3ONO^* \rightarrow CH_3O + NO. \quad (R1)$$

Earlier reports showed that the primary photodissociation channel upon UV excitation produced CH_3 radicals and NO_2, after which the NO_2 may absorb another photon leading to formation of NO and O radical:

$$CH_3NO_2 + hv \rightarrow CH_3 + NO_2. \quad (R2)$$

Based upon RRKM modeling and the assumed IRMPD kinetics, Wodtke *et al.* concluded the energy barrier for isomerization was about 5 kcal/mol lower than the C−N bond fission threshold.[20] This would certainly justify the observation of a significant yield of the products from the isomerization channel. This report triggered a series of theoretical calculations on the dissociation dynamics of nitromethane performed by several groups.[21–23] However, none of them could establish the dissociation mechanism via isomerization as an energetically favorable pathway. However, McKee[24] and Saxon[25] *et al.* did identify a loose transition state leading to the isomerization channel, but at significantly higher energies compared to the radical dissociation pathway. Finally, in 2009, Zhu and Lin[16] revisited the calculations on nitromethane decomposition and located the presence of a loose transition state just below the C−N dissociation limit. The structure of the loose transition state in the isomerization pathway was found to have a striking resemblance to the roaming pathway in the photodissociation of H_2CO.[26] Recently, Homayoon and Bowman[15] performed quasiclassical trajectory (QCT) calculations using a global potential energy surface (PES) for nitromethane decomposition that theoretically documented the roaming-mediated isomerization of $CH_3NO_2 \leftrightarrow$ *cis*-CH_3ONO. Similar behavior had been inferred in the UV photodissociation of nitrobenzene based on ion imaging and statistical modeling of the product branching and translational energy release on the ground and first triplet excited states.[13] Several features of this isomerization pathway justify the use of the phrase "roaming-mediated":[15] (1) it involves nuclear reorientation dynamics that take place at long-range (3–5 Å) and that have an energetic threshold within 1–2 kcal/mol of a bond fission asymptote and (2) trajectory calculations show that this TS is indeed very loose and many trajectories do not go very near this precise configuration.

The study of photodissociation using ion-imaging was introduced in late 1980s[27] and was later developed into high resolution velocity map imaging by Eppink and Parker[28] and DC slice imaging in our group.[29] Imaging provides the complete velocity and angular distribution of the products formed, generally with quantum state selectivity and excellent sensitivity. Since the last decade, velocity map imaging studies have been used extensively in studying the photochemistry of unimolecular dissociation and scattering.[30,31] The present article demonstrates the first imaging studies combining IRMPD with state-selected imaging. Our focus is on the ground state photodissociation dynamics of nitromethane and methyl nitrite (CH_3ONO). The results provide further support to the recent theoretical studies that propose roaming-mediated isomerization in nitromethane and are in good agreement with the earlier results of Wodtke, Hintsa, and Lee.

EXPERIMENTAL

A detailed description of the DC sliced imaging technique used in this experiment is described in Ref. 29. The carrier gas helium is bubbled through a sample of nitromethane producing a seeded mixture of 3% nitromethane in He. Likewise, in case of methyl nitrite, helium was passed through a bubbler maintained at 196 K forming a ratio of 2% methyl nitrite in He. Methyl nitrite was synthesized by adding 15 ml of methanol to a solution of 12 g of $NaNO_3$ dissolved in 50 ml of deionized water and stirred at room temperature for 5 min. To the resulting solution concentrated HCl was added dropwise through a separating funnel. Methyl nitrite vapors were formed as white fumes, which were condensed to a dark yellow liquid in a bubbler, kept in dry ice/acetone cooling bath (196 K).

The molecular beam was generated by supersonic expansion into the source chamber through pulsed nozzle (General Valves series 9) of diameter 0.3 mm. The pulsed nozzle is fitted to a copper tube having a bore diameter of 0.5 mm that is heated to 573 K which facilitates the population of a few vibrational levels of the ground state to promote IR absorption. The expanded beam was introduced into the interaction chamber through a skimmer of 1 mm diameter and entered the DC sliced imaging ion optics assembly comprising four electrodes where it intersected two counter-propagating laser beams. The pressure inside the source chamber and the interaction chamber was maintained at 1×10^{-5} Torr and 1×10^{-7} Torr, respectively. On entering the detection chamber the molecular beam interacts with the CO_2 laser beam and the UV beam at ~226 nm. Absorption of many photons from the IR beam from a line-tunable TEA-CO_2 laser leads to dissociation of the molecule on the ground electronic state. The CO_2 laser lines selected for nitromethane and methyl nitrite were 9.6 μm [R(20) line] and 10.2 μm [R(32) line], respectively. Following dissociation, the fragment is state-selectively ionized with the 226 nm beam which was generated from the fundamental output of a pulsed dye laser (Sirah, DCM dye in ethanol) pumped by the second harmonic of a seeded Nd: Yttrium aluminum garnet (Nd:YAG) laser (Quanta Ray, Spectra Physics) which is then mixed with the third harmonic of the Nd:YAG laser. The intensity of the 226 nm beam was reduced to 200 μJ/pulse to eliminate the contribution from photodissociation at 226 nm. The typical energy produced by the CO_2 laser was 100 mJ/pulse and the laser was operated at a frequency of 10 Hz. Both the beams were aligned in the counter-propagating manner and the IR beam was focused onto the molecular beam with a 450 mm focal length ZnSe lens but the UV beam at 226 nm was left unfocused with a diameter of ~5 mm. The temporal overlap between the two laser beams was controlled through a digital delay generator. The CO_2 laser beam was introduced into the chamber 1.2 μs prior to the UV beam. The ions originating from the interaction of the laser beams with the molecular beam were directed through the time-of-flight tube and detected by a 120 mm microchannel plate detector coupled with a fast phosphor

screen. The ion image was captured using a USB CCD camera (USB 2 uEye SE, IDS) and the acquisition was done using our own NuACQ program. The acquired image was analyzed using in-house software to obtain the translational energy distribution for the various rotational levels. The IRMPD REMPI scan was recorded by scanning the UV laser and monitoring the ion signal on the phosphor screen with a photomultiplier tube (PMT). The signal from the PMT was transferred to the PC through an oscilloscope. The REMPI spectrum was generated by acquiring the signal with a custom LabView program.

QUASICLASSICAL TRAJECTORY CALCULATIONS

Details concerning the global potential energy surfaces for CH_3NO_2 have been published previously,[21] so only a short summary of those is given here. The PES is a permutationally invariant representation of 114000 DFT/B3LYP energies and precisely reproduces the reaction paths. Fig 1 shows the relevant pathways for NO production from nitromethane and methyl nitrite. TS1 is the loose "roaming" saddle point (SP) that connects CH_3NO_2 to *cis*-CH_3ONO. We note that the importance of a roaming-like transition state in nitromethane was first invoked by Lin[16] to resolve a long-standing discrepancy between experiment and theory on nitromethane decomposition, and subsequently characterized rigorously in Ref. 21. It was shown in that work that isomerization trajectories involved average C–N bond distances of more than 4 Å and vibrational frequencies essentially matching those of CH_3 and NO_2, clearly justifying its characterization as a roaming TS. Although a higher energy tight TS to *trans*-CH_3ONO (and then without potential barrier to $CH_3O + NO$) was found, it is expected to play a negligible role because it is both energetically and entropically disfavored. It is shown as TS3 in Fig. 1. Cis- and *trans*-CH_3ONO isomerization takes place via TS2. Finally $CH_3O + NO$ products are from O–N bond dissociation of CH_3ONO.

Twenty thousand trajectories were run initiated at *cis*-CH_3ONO at 5 kcal mol^{-1} relative to the harmonic ZPE of $CH_3O + NO$. Initial conditions were generated using microcanonical sampling of the initial kinetic energy and with the constraint of zero total angular momentum. Trajectories were run with a maximum of 1 000 000 steps with 0.097 fs step-size. The trajectories were terminated when one of the internuclear distances became larger than 20 bohrs. In the QCT calculations, ZPE issues for the products need to be addressed. Here we adopt the "hard-constraint" in which trajectories are discarded if either fragments NO or CH_3O is formed with less than the ZPE. In addition, we report the vibrational energy distribution of the CH_3O product for trajectories initiated at nitromethane and *cis*-methyl nitrite with the same total energies for two different energies. Two batches of 20 000 trajectories were run at 60.1 and 86.1 kcal mol^{-1} energy above the harmonic ZPE of *cis*-CH_3ONO. In the "Results and discussion" section, the vibrational energy distribution of CH_3O from these trajectories is compared with the results of CH_3O fragments from CH_3NO_2 at the same energies. (The translational energy distribution of trajectories initiated at CH_3NO_2 has been reported in Ref. 15.)

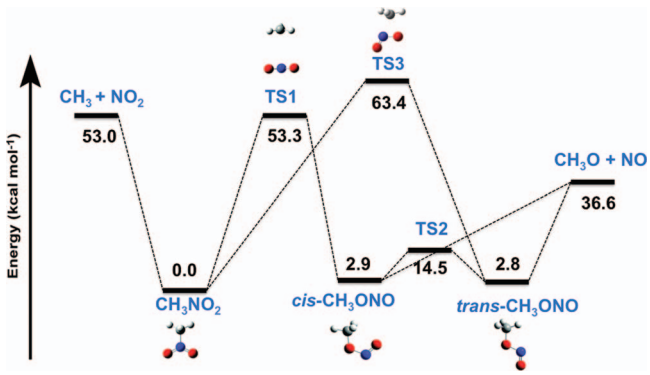

FIG. 1. Stationary points for different isomerization/dissociation pathways of CH_3NO_2 leading to $CH_3O + NO$. The energies for the different states are shown relative to the CH_3NO_2 minimum.

RESULTS AND DISCUSSION

The schematic of the PES for the isomerization and dissociation pathways of nitromethane and methyl nitrite obtained by Homayoon and Bowman[15] are shown in Figure 1. The energies of the various states are shown relative to the global minimum of nitromethane and the energies are not corrected for zero point energy. The schematic shows that the loose transition state leading to isomerization to *cis*-methyl nitrite is almost isoenergetic with the radical dissociation limit, as is typical for a "roaming" type transition state. This is indicative that a fair amount of branching to the isomerization channel is possible if nitromethane is excited near the dissociation threshold. A REMPI spectrum was recorded for nitromethane on the 0–0 band for the $A(^2\Sigma^+) \leftarrow X(^2\Pi_r)$ transition for the NO and is shown in Figure 2. The spectrum displayed in the region 44 180–44 300 cm^{-1} shows numerous peaks that reflect the rotational distribution of the NO fragment upon dissociation. The peaks are assigned to each rotational transition by comparing the exact position to the simulated spectrum of NO obtained from the LIFBASE program.[32] Intense peaks in the lower energy region of the band (44 195–44 245 cm^{-1}) suggest larger population in the lower rotational levels as expected from IRMPD. The intensities of the isolated spectral lines for the Q and R branch were integrated and divided by the state degeneracy factor $(2J + 1)$, which produced the population of individual states. The logarithm of the population densities for the different rotational levels $P(J)/(2J + 1)$ was plotted against internal energy (E_{int}) and the result is shown in Figure 3. A Boltzmann rotational distribution would be described by the equation $P(J) \sim \exp[-E_{int}(J)/kT_{Rot}]$, so the slope in Fig. 3 gives the rotational temperature (T_{Rot}) of the photofragments. The three lowest rotational levels show an elevated population possibly reflecting NO contamination in the beam, and these are excluded from the Boltzmann fit. The rotational temperature (T_{Rot}) of the products obtained from the Q and R branches are 513 K and 411 K, but we emphasize that there is no reason the rotational distributions must exhibit a well-defined temperature. Dissimilar rotational temperatures for the Q and R branch implies that higher rotational levels are differentially populated which denotes preferential occupancy of specific

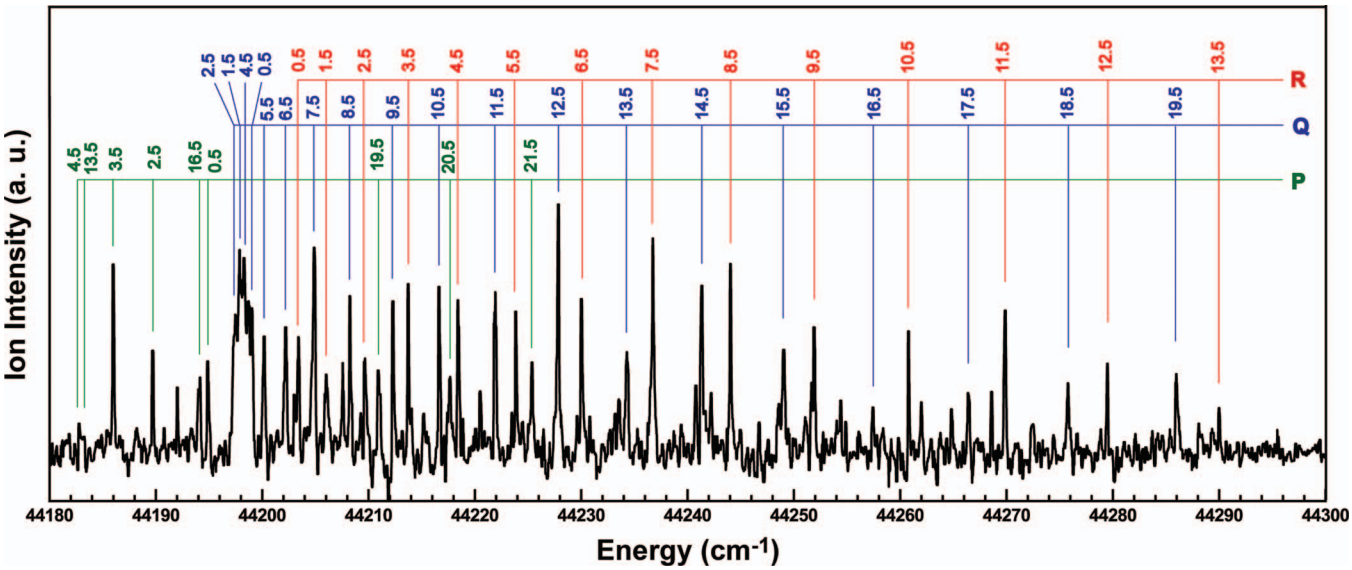

FIG. 2. Rotationally resolved resonant multiphoton ionization spectrum of nascent NO formed from the IRMPD of nitromethane. The peaks are fitted to the rotational lines for the $A(^2\Sigma^+) \leftarrow X(^2\Pi_r)$ transitions acquired from the LIFBASE program.[28]

Λ-doublet states. This is confirmed by comparing the intensities of the lines as well as the images, as discussed below.

The velocity distribution of the products resulting from IRMPD of nitromethane was obtained from the DC sliced images of the photofragments. DC sliced images of NO fragments were recorded from IRMPD of nitromethane for the Q and R branches for different rotational levels are shown in Figure 4. The images recorded for the nascent NO fragments for different J values probed around 226 nm show only a single component. The brighter regions of the image correspond to higher intensity of the products and the distance from the center of the image gives a measure of recoil velocity of the products. The total translational energies were calculated using conservation of energy and momentum (assuming CH_3O as co-fragment) and the images are displayed alongside. A greater intensity is observed in the images for NO probed via the Q-branch than the R-branch. This disparity indicates that the dissociation favors formation of NO with the π orbital perpendicular to the plane of rotation as discussed further below. The total translational energy distributions for nitromethane show that the energies peak near zero, suggesting barrierless dissociation. Theoretical calculations reveal that methyl nitrite undergoes barrierless decomposition upon isomerization from nitromethane.[15,16] The average experimentally determined translational energy

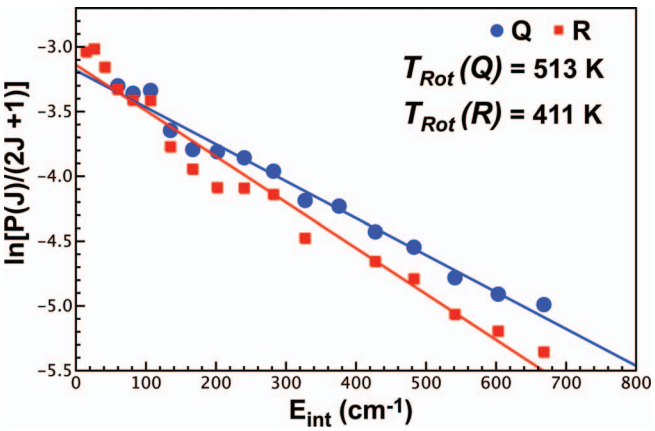

FIG. 3. Product state distributions for the Q and R branches at different rotational levels of NO obtained from the IRMPD of nitromethane. These are fitted to a Boltzmann distribution to obtain the rotational temperature (T_{Rot}).

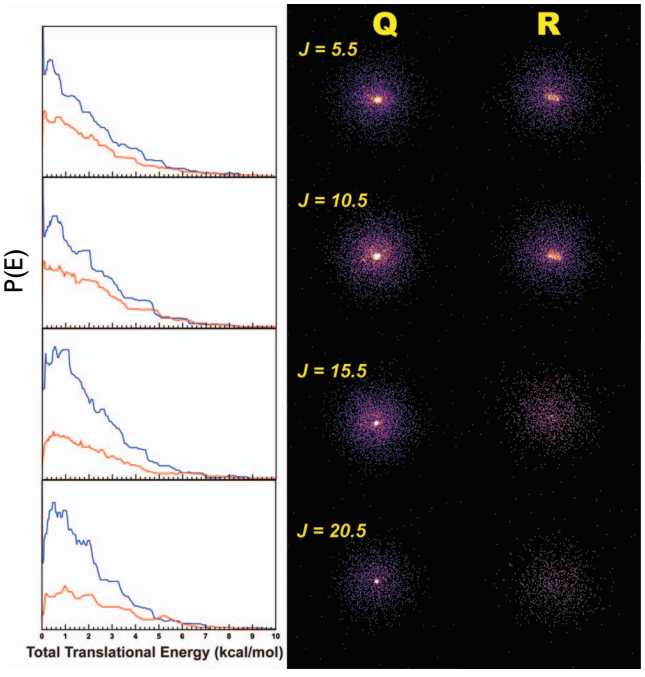

FIG. 4. Direct current sliced images of NO obtained from IRMPD of nitromethnane. Nitromethane was dissociated by setting the CO_2 laser at 9.6 μm and NO was probed around 226 nm. The images were recorded for Q and R branches of different rotational levels which highlights the notable difference in their intensities. (Left) The center-of-mass total translational energies of the fragments for different states of Q (blue) and R (red) branches are also presented.

TABLE I. Average total translational energy values (in kcal/mol) for the Q to R branches at different rotational levels of nitromethane and methyl nitrite.

	Nitromethane (CH_3NO_2)		Methyl nitrite (CH_3ONO)	
J value	Q	R	Q	R
5.5	3.3	2.2	1.6	1.4
10.5	3.1	2.4	1.8	1.5
15.5	5.4	2.5	1.1	1.2
20.5	4.7	2.6	0.8	1.2

release ranges from 3.3 kcal/mol to 5.4 kcal/mol for the Q-branch and ranges from 2.2 to 2.6 kcal/mol for the R-branch (see Table I). The limiting value for the total translational energy was found to be ∼8 kcal/mol, which is in agreement with the results of the similar IRMPD studies of Lee and co-workers.[20] The present IRMPD results are also consistent with the QCT calculations on nitromethane that show the limiting value for the total translation energy of the products to be ∼10 kcal/mol at the dissociation threshold (Fig. 4 in Ref. 14). Calculations done by Zhu and Lin[16] suggested that the roaming mediated isomerization channel dominates at the dissociation threshold, which was later confirmed by the QCT calculations by Homayoon and Bowman.[15] Their branching ratio indicates that NO is the exclusive product via the isomerization channel at the dissociation threshold, with increasing contributions from the radical dissociation channel at higher energies.[15] Observation of a single component in the images also implies that NO is produced from a single channel. Examination of trajectories reveals a roaming/isomcrization pathway[15] that passes near the saddle-point transition state (TS1). On this pathway, the NO_2 fragment moves far from CH_3 (to C–N distances as large 4.6 Å[15]) and reorients itself and visits the region of isomerization to cis-CH_3ONO followed by O-atom transfer. Evidence of roaming dynamics in formation of NO from photodissociation of NO_3 from both ground and excited state has also been recently reported.[33]

One interesting question to contemplate is whether the interaction of the IR beam with the hot molecule could influence the outcome, i.e., whether some subset of the sampled phase space could preferentially absorb additional IR photons, promoting dissociation via specific paths. In general such issues may be neglected because an energized molecule will spend that bulk of its time with relatively low excitation in any particular mode. During roaming events, however, the molecule may spend a relatively long time in a particular "excursion," perhaps on the order of 10^{-12} s at most. Although this is still very short compared to the lifetime of the system, if the molecule were to absorb very strongly from these geometries, some distortion of the outcome is conceivable. In the present case, however, the roaming geometries will fall out of resonance with the CO_2 laser, (CH_3 and NO_2 have no absorptions in this region) so no effect is expected. This *attenuation* of absorption during a roaming event could not significantly influence the outcome because the molecule spends only a small fraction of its time in the roaming geometry (or in any TS configuration).

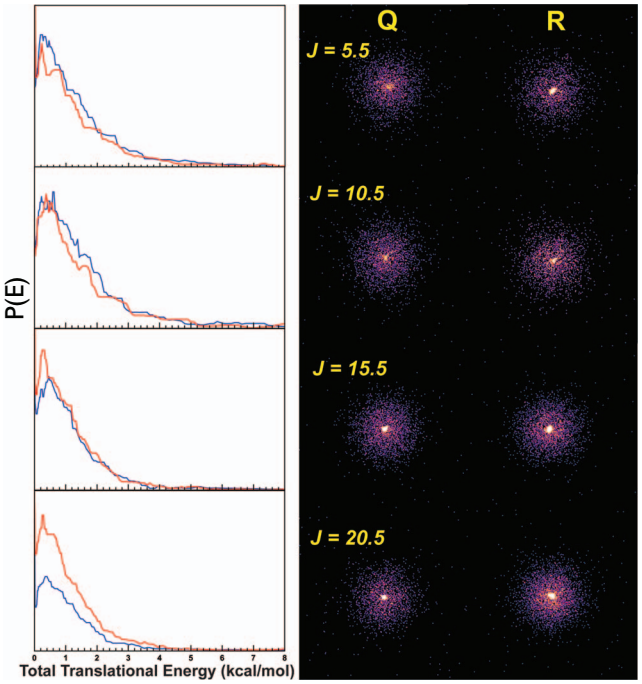

FIG. 5. Direct current sliced images of NO obtained from IRMPD of methyl nitrite. Methyl nitrite was dissociated by setting the CO_2 laser at 10.2 μm and NO was probed around 226 nm. The images were recorded for Q and R branches of different rotational levels. (Left) The center-of-mass total translational energies of the fragments for different states of Q (blue) and R (red) branches are also presented.

IRMPD of methyl nitrite was carried out for comparison with the results obtained from nitromethane. The DC sliced images of IRMPD of methyl nitrite were recorded for the various rotational levels and are shown in Figure 5. The images of NO observed from methyl nitrite look similar to those of nitromethane. The total center-of-mass translational energy for the photofragments was calculated using the conservation of momentum and are displayed alongside images in Figure 5. The curves show the total translational energy extending up to 5 kcal/mol and peaking at around 0 kcal/mol. The low translation energy release of the products is expected as the dissociation of methyl nitrite occurs through a simple fission of O−N bond. The potential energy diagram in Figure 1 depicts that both the *cis* and *trans* isomers of methyl nitrite undergo barrierless decomposition into CH_3O and NO. The experimental values for the total translational energy show a close resemblance when compared with the calculated total translational energy curve for the CH_3O and NO fragments obtained in trajectory calculations displayed in Figure 6. The trajectory data shows a peak at ∼1.5 kcal/mol, a limiting value of 4.5 kcal/mol, and an average translational energy release of 1.7 kcal/mol. The total translational energies are calculated at 5 kcal/mol above the NO asymptote. Dissociation of methyl nitrite from the ground state proceeds through a simple bond rupture leading to very low translational energy release. The average translational energy observed for the fragments originating from the IRMPD of nitromethane is higher when compared with methyl nitrite. As seen from the PES in Figure 1, nitromethane has to overcome the energy barrier for isomerization which provides substantial internal energy to

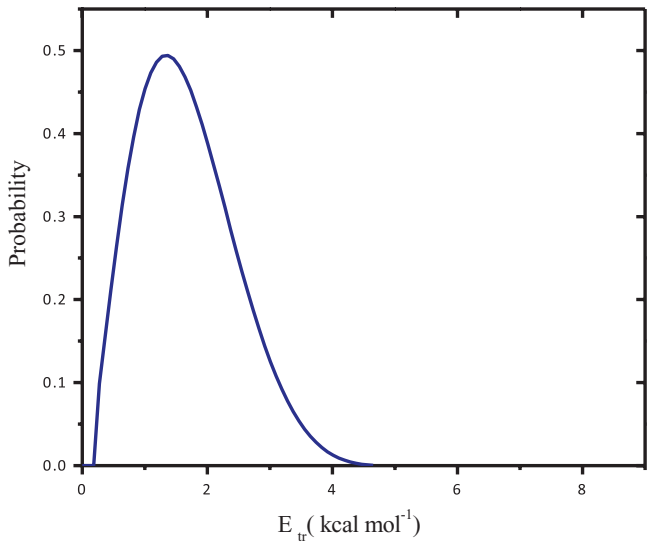

FIG. 6. Total translational energy distribution of the products formed from dissociation of CH_3ONO to CH_3O and NO from the QCT calculations. The translational energy was calculated at 5 kcal/mol above the dissociation limit.

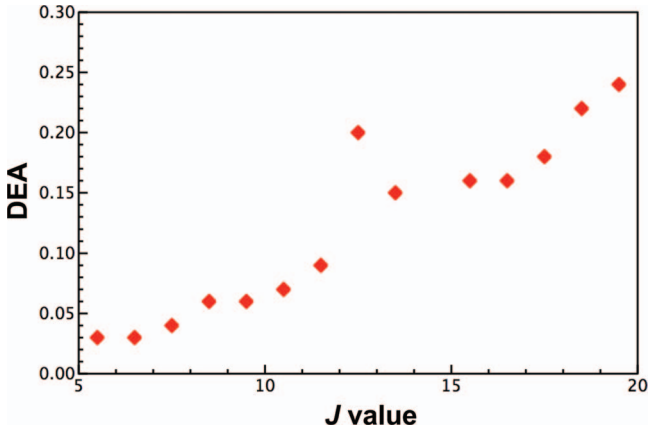

FIG. 7. Plot of degree of electron alignment against total angular momentum (J) for IRMPD of nitromethane.

the isomerized methyl nitrite. The isomerized methyl nitrite later dissociates and the energy is in part released in the form of translational energy of the products. Recently, Lin and co-workers studied the thermal decomposition of methyl nitrite and found another competitive pathway resulting in formation of CH_2O and HNO.[34] Their calculations located another roaming transition state 0.7 kcal/mol below the $CH_3O + NO$ asymptote. Future plans are made to study the CH_2O and HNO fragments which can be detected with the newly built Chirped-Pulse FT-microwave spectrometer in our lab.

Formation of Λ-doublet states are observed in photoproducts containing diatomic molecules with an unpaired electron such as NO.[35] A Λ-doublet propensity indicates that the fragment retains stereochemical information about the bond that is broken in dissociation, and it is reflected in the orientation of the orbital relative to the rotation of the diatomic fragment. In the present article, the states are depicted following the notation used by Alexander *et al.*[36] The two states are denoted by $\Pi(A'')$ and $\Pi(A')$ in which the unpaired electron in the π orbital is either aligned parallel to J or resides in the plane of rotation of the molecule respectively. Spectroscopically, the populations of the two Λ-doublet states can be probed by measuring the relative population through different rotational branches although the actual energy splitting between the states is quite small. The $\Pi(A'')$ state is sensitive to the Q branch and $\Pi(A')$ state is sensitive to the P (or R) branch.[37]

The orbital alignment for the nascent NO products can also be expressed in terms of degree of electron alignment (DEA) as $(\Pi(A'') - \Pi(A'))/(\Pi(A'') + \Pi(A'))$. For a complete orbital alignment of the products, DEA = 1. We can use the REMPI spectrum recorded for nitromethane IRMPD in Fig. 2 to obtain the Λ-doublet propensities. The DEA for the products was calculated by integrating the area under the peaks for transitions of Q and R branch from the spectrum. The plot of DEA against J value is shown in Figure 7. The plot shows that the DEA value steadily increases from 0.03 to 0.24 with increasing J values. There is a single outlier at $J = 12.5$ which resulted probably from the intensity fluctuation of the probe laser. This implies that at higher J values, the $\Pi(A'')$ state is significantly more populated. Therefore, it is evident that the dissociation from CH_3NO_2 via TS1 occurs through a planar framework and post-dissociation, the unpaired electron in the pπ orbital is preferentially aligned parallel to J in the nascent NO fragments.

In contrast to this, careful IRMPD studies on methyl nitrite by King and Stephenson show the absence of a Λ-doublet propensity.[38] Integration of our images in Figs. 4 and 5 may also be used to explore the Λ-doublet propensities, and these are consistent with the results in Fig. 7 and those of King and Stephenson, i.e., a significant Λ-doublet propensity is seen for IRMPD of nitromethane, while none is seen for methyl nitrite IRMPD. Earlier, the UV photodissociation dynamics of methyl nitrite and its Λ-state populations were studied extensively using one-photon[39] or two-photon[40,41] LIF. These studies established that dissociation occurs through a planar CONO framework with the unpaired electron preferentially residing in the pπ orbital parallel to J. A remarkable bimodal Λ-doublet propensity was observed in "roaming" mediated dissociation of NO_3 by North and co-workers.[33] In that case, the nascent NO fragment showed opposite alignment of the pπ orbital for dissociation of NO_3 originating from the ground and excited state.

These results suggest two possibilities: the Λ-doublet propensity seen in IRMPD of nitromethane may be a signature of the roaming pathway and the transition state TS1, giving rise to dissociation from restricted geometries and a nonstatistical product state distribution. Alternatively, the difference might simply reflect the different available energies, as IRMPD from nitromethane necessarily occurs at a significantly higher energy relative to the global minimum compared to methyl nitrite. We have examined the vibrational excitation in the methoxy radical product in the trajectory calculations to gain insight into this question. We have initiated these trajectories at two energies starting either at the global minimum (nitromethane) or at *cis*-methyl nitrite. The results, shown in Fig. 8, reveal sharp differences: the methoxy product formed via TS1 shows the substantial vibrational excita-

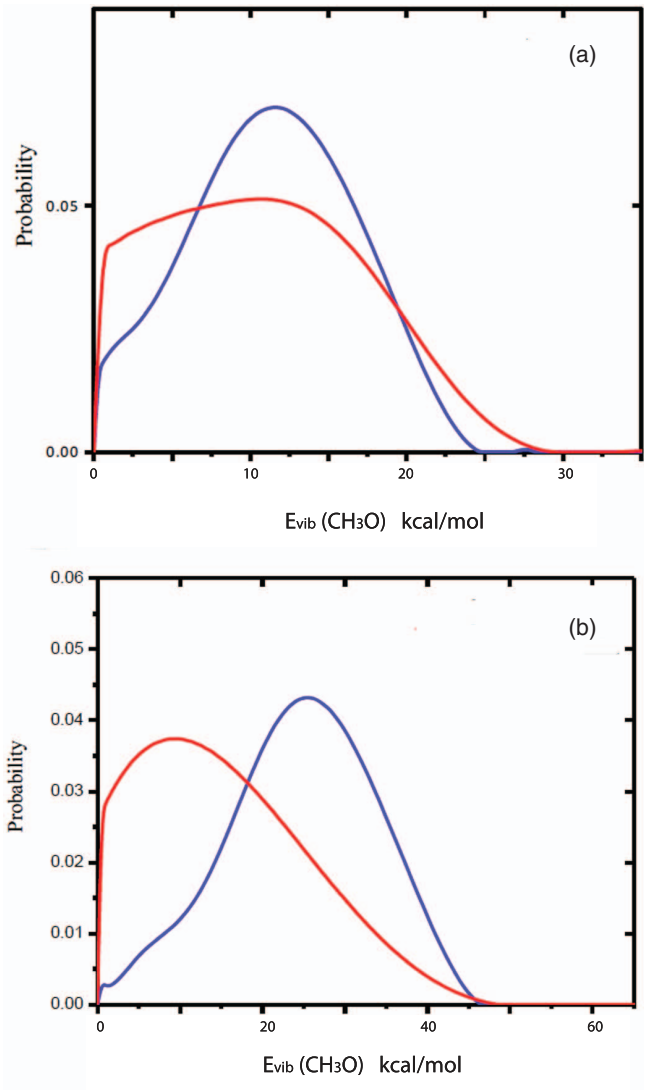

FIG. 8. Methoxy radical vibrational energy content for trajectories initiated at the nitromethane global minimum (blue curves) or at the *cis*-methyl nitrite minimum (red curves). (a) Total energy 63 kcal/mol and (b) total energy 89 kcal/mol.

tion often seen in the new bond in a roaming event, while the methyl nitrite case appears fully statistical. This strongly suggests that the passage over TS1 gives rise to a nonstatistical product state distribution and preserves memory of the CONO plane in the subsequent dissociation, with a corresponding Λ-doublet propensity. A rigorous comparison of methoxy internal excitation to experiment is not possible because the precise experimental excitation energy is not known, nor is the full NO internal state distribution measured here. However, if we make the reasonable assumptions that the dissociation is near threshold and the NO product distribution is primarily in $v = 0$, then we infer that ~14 kcal/mol is in methoxy internal excitation, and this must largely be vibration owing to angular momentum constraints. If the excitation is further above threshold then any additional excitation energy must also reside in methoxy internal excitation, so this 14 kcal/mol is a lower bound.

We note at the higher energy a pathway to *trans*-CH_3ONO via the tight saddle point[15,16,21] (TS3) is classically energetically open. Dissociation from *trans*-CH_3ONO to $CH_3O + NO$ is then possible via the conventional pathway indicated in Figure 1. We have not investigated the fraction of trajectories that may produce $CH_3O + NO$ via TS3 at the higher energy. However, based on both the lower energy and the "floppiness" of the roaming pathway we expect it to be dominant pathway even at the higher energy. We investigated this by running 2000 trajectories from TS3 at this higher energy and observed that the CH_3O vibrational distribution peaks at roughly 20 kcal/mol. This is 10 kcal/mol below the peak in the distribution seen in the lower panel of Figure 8 for trajectories initiated at the NM global minimum. Thus, this supports the statement that this tight saddle-point pathway is playing a minor role at this higher energy and further supports the methoxy vibration as a "signature" of the roaming pathway in this case.

CONCLUSION

To our knowledge this is the first study to combine IRMPD with state selective ion imaging. This approach can provide useful information about the dynamics of unimolecular reactions near threshold that originate from the ground state, features that are particularly relevant for reactions involving "roaming" pathways. IRMPD imaging studies of nitromethane show very low translational energy release of the photofragments and reiterated the importance of "roaming" pathway in the dissociation of nitromethane. These findings are in good agreement with the QCT calculations[15] and the IRMPD studies of Wodtke *et al.*[20] From the intensities of the images and recorded IRMPD REMPI spectrum, we find that the A″ Λ-doublet state is more populated. Considering the dissociation to have a planar geometry, it is observed that post-dissociation the unpaired electron preferably stays in the $p\pi$ orbital perpendicular to the plane of rotation. In contrast, dissociation of methyl nitrite does not show any Λ-doublet propensity. Significant differences in the methoxy internal state distributions in QCT calculations for nitromethane and methyl nitrite at the same total energy suggest that the Λ-doublet propensity and the methoxy vibrational excitation are both signatures of the roaming-mediated isomerization, with fairly rapid decomposition following isomerization precluding full intramolecular vibrational energy redistribution.

ACKNOWLEDGMENTS

A.G.S. acknowledges the Army Research Office Award No. 58245-CH-11 for financial support and J.M.B. acknowledges the Army Research Office Award No. (W911NF-11-1-0477) for financial support.

[1]N. R. Isenor and M. C. Richardson, Appl. Phys. Lett. **18**, 224 (1971).
[2]D. S. Bomse and J. L. Beauchamp, J. Am. Chem. Soc. **102**, 3967 (1980).
[3]D. S. Bomse, D. W. Berman, and J. L. Beauchamp, J. Am. Chem. Soc. **103**, 3967 (1981).
[4]D. P. Little, J. P. Speir, M. W. Senko, P. B. O'Connor, and F. W. McLafferty, Anal. Chem. **66**, 2809 (1994).
[5]C. L. Berrie, C. A. Longfellow, A. G. Suits, and Y. T. Lee, J. Phys. Chem. A **105**, 2557 (2001).
[6]C. A. Longfellow and Y. T. Lee, J. Phys. Chem. **99**, 15532 (1995).

[7]E. J. Hintsa, A. M. Wodtke, and Y. T. Lee, J. Phys. Chem. **92**, 5379 (1988).
[8]P. A. Schulz, A. S. Sudbø, D. J. Krajnovich, H. S. Kwok, Y. R. Shen, and Y. T. Lee, Annu. Rev. Phys. Chem. **30**, 379 (1979).
[9]A. S. Sudbø, P. A. Schulz, Y. R. Shen, and Y. T. Lee, in *Multiple-Photon Excitation and Dissociation of Polyatomic Molecules*, edited by C. Cantrell (Springer, Berlin, 1986), Vol. 35, p. 95.
[10]J. M. Bowman and B. C. Shepler, Annu. Rev. Phys. Chem. **62**, 531 (2011).
[11]N. Herath and A. G. Suits, J. Phys. Chem. Lett. **2**, 642 (2011).
[12]D. Townsend, S. A. Lahankar, S. K. Lee, S. D. Chambreau, A. G. Suits, X. Zhang, J. Rheinecker, L. B. Harding, and J. M. Bowman, Science **306**, 1158 (2004).
[13]M. L. Hause, N. Herath, R. Zhu, M. C. Lin, and A. G. Suits, Nat. Chem. **3**, 932 (2011).
[14]Z. Homayoon, J. M. Bowman, A. Dey, C. Abeysekera, R. Fernando, and A. G. Suits, Z. Phys. Chem. **227**, 1267 (2013).
[15]Z. Homayoon and J. M. Bowman, J. Phys. Chem. A **117**, 11665 (2013).
[16]R. S. Zhu and M. C. Lin, Chem. Phys. Lett. **478**, 11 (2009).
[17]L. J. Butler, D. Krajnovich, Y. T. Lee, G. S. Ondrey, and R. Bersohn, J. Chem. Phys. **79**, 1708 (1983).
[18]D. B. Moss, K. A. Trentelman, and P. L. Houston, J. Chem. Phys. **96**, 237 (1992).
[19]Y. Q. Guo, A. Bhattacharya, and E. R. Bernstein, J. Phys. Chem. A **113**, 85 (2009).
[20]A. M. Wodtke, E. J. Hintsa, and Y. T. Lee, J. Phys. Chem. **90**, 3549 (1986).
[21]M. L. McKee, J. Am. Chem. Soc. **108**, 5784 (1986).
[22]M. T. Nguyen, H. T. Le, B. Hajgató, T. Veszprémi, and M. C. Lin, J. Phys. Chem. A **107**, 4286 (2003).
[23]W.-F. Hu, T.-J. He, D.-M. Chen, and F.-C. Liu, J. Phys. Chem. A **106**, 7294 (2002).
[24]M. L. McKee, J. Phys. Chem. **93**, 7365 (1989).
[25]R. P. Saxon and M. Yoshimine, Can. J. Chem. **70**, 572 (1992).
[26]S. A. Lahankar, S. D. Chambreau, D. Townsend, F. Suits, J. Farnum, X. Zhang, J. M. Bowman, and A. G. Suits, J. Chem. Phys. **125**, 044303 (2006).
[27]D. W. Chandler and P. L. Houston, J. Chem. Phys. **87**, 1445 (1987).
[28]A. T. J. B. Eppink and D. H. Parker, Rev. Sci. Instrum. **68**, 3477 (1997).
[29]D. Townsend, M. P. Minitti, and A. G. Suits, Rev. Sci. Instrum. **74**, 2530 (2003).
[30]N. Hansen, A. M. Wodtke, A. V. Komissarov, K. Morokuma, and M. C. Heaven, J. Chem. Phys. **118**, 10485 (2003).
[31]H. A. Cruse and T. P. Softley, J. Chem. Phys. **122**, 124303 (2005).
[32]J. Luque and D. R. Crosley, LIFBASE: Database and spectral simulation program, version 1.6, SRI International Report MP, 1998.
[33]M. P. Grubb, M. L. Warter, H. Xiao, S. Maeda, K. Morokuma, and S. W. North, Science **335**, 1075 (2012).
[34]R. S. Zhu, P. Raghunath, and M. C. Lin, J. Phys. Chem. A **117**, 7308 (2013).
[35]R. S. Mulliken and A. Christy, Phys. Rev. **38**, 87 (1931).
[36]M. H. Alexander, P. Andresen, R. Bacis, R. Bersohn, F. J. Comes, P. J. Dagdigian, R. N. Dixon, R. W. Field, G. W. Flynn, K. H. Gericke, E. R. Grant, B. J. Howard, J. R. Huber, D. S. King, J. L. Kinsey, K. Kleinermanns, K. Kuchitsu, A. C. Luntz, A. J. McCaffery, B. Pouilly, H. Reisler, S. Rosenwaks, E. W. Rothe, M. Shapiro, J. P. Simons, R. Vasudev, J. R. Wiesenfeld, C. Wittig, and R. N. Zare, J. Chem. Phys. **89**, 1749 (1988).
[37]P. Andresen and E. W. Rothe, J. Chem. Phys. **82**, 3634 (1985).
[38]D. S. King and J. C. Stephenson, J. Chem. Phys. **82**, 2236 (1985).
[39]C. G. Atkins and G. Hancock, Laser Chem. **9**, 195 (1988).
[40]F. Lahmani, C. Lardeux, and D. Solgadi, Chem. Phys. Lett. **129**, 24 (1986).
[41]U. Bruhlmann, M. Dubs, and J. R. Huber, J. Chem. Phys. **86**, 1249 (1987).